

Electrochemical properties of LiMnBO₃ as a potential cathode material for lithium batteries

Y.-S. Lee^a and H. Lee^{b,*}

^aSchool of Materials Science and Engineering, Andong National University, Andong 760-742, Korea

^bMaterials Research Center for Energy and Green Technology, Andong National University, Andong 760-745, Korea

Pristine LiMnBO₃ and carbon incorporated LiMnBO₃ are synthesized by a simple solid state reaction at 500 or 800 °C. For carbon incorporation, ketchen black or sucrose are added in the starting powder as a carbon source. While the pristine LiMnBO₃ shows very small specific capacities at both temperatures, the added carbon into LiMnBO₃ substantially increases the capacity up to 76 mAh/g at the 30th cycle. Firing at 500 and 800 °C results in monoclinic and hexagonal phases, respectively, and the monoclinic LiMnBO₃ addresses better electrochemical properties in terms of the specific capacity and cycling performance.

Key words: LiMnBO₃, Carbon, Capacity, Lithium ion batteries.

Introduction

Historically, the cathode material for Li-ion batteries has been layered oxides, such as LiCoO₂ or LiNi_{0.33}Mn_{0.33}Co_{0.33}O₂, due to their high capacity, excellent cycle characteristics, and high energy density [1]. Nevertheless, their high toxicity, high cost, and instability at high temperature have prohibited them from the large scale use and, thereby, foster the search of alternative cathode materials to meet the requirement for new applications like electric vehicle, power storage for smart grid, etc. [2-8]. The most notable alternative cathode material to date is LiFePO₄ [2]. LiFePO₄ has olivine-type structure, which allows fast ion transport and excellent thermal stability from its three-dimensional frame made up of the PO₄ tetrahedra and MO₆ octahedra. Furthermore, the inductive effect from polyanion increases the redox potential of Fe³⁺/Fe²⁺ couple significantly, yielding higher cell voltage [8, 9]. One drawback of LiFePO₄ is, however, low energy density due to its relatively low cell voltage (~3.3 V) and capacity (~170 mAh/g). Thus, much attention has been focused on other polyanion-based materials such as LiMnPO₄ [10, 11], silicates (Li₂MSiO₄) [12, 13], and borates (LiMBO₃) [14-15].

Among those polyanion-based materials, borates possess very low molecular weight and high electronegativity, which suggest that borate electrode materials can have high gravimetric capacity and strong inductive effect for larger cell voltage. After the first investigation on the Li-ion intercalation behavior of some borate materials

(LiMBO₃, M = Fe, Mn, and Co) [14], only a handful of studies have been conducted on borate-based electrode materials [15-19]. Like other polyanion-based electrode materials, LiMBO₃ has inherent low electronic conductivity, so that the aid for enhancing the electronic conductivity is required. In this regard, the incorporation of carbon in the polyanion-based electrode materials has been very successful [5-9] and a recent study reported the capacity of > 190 mAh/g of LiFeBO₃/C composite cathode [15,16]. Thus, there is a potential for LiMBO₃ being a new cathode material with high energy.

The present study is a part of a work which aims to investigate the potential of borate-based materials as a cathode material, and the preliminary results on LiMnBO₃ are presented here. LiMnBO₃ has a theoretical capacity of 222 mAh/g and a potentially higher redox potential of Mn³⁺/Mn²⁺ than that of Fe³⁺/Fe²⁺ in LiFeBO₃. In this study, pristine LiMnBO₃ and carbon incorporated LiMnBO₃ were synthesized by a simple solid state reaction and their lithium electrochemical properties were measured and analyzed.

Experimental

Pristine LiMnBO₃ powder was prepared by a simple solid state reaction of stoichiometric amounts of Li₂CO₃, MnCO₃, and H₃BO₃. The mixture were dispersed into acetone, ball milled for 12 hrs in a planetary mill with a rotating speed of 250 rpm, and then vacuum dried at 60 °C for 24 hrs. After the complete evaporation of acetone, the resulting powder was fired at 500 or 800 °C for 10 hrs in Ar-flowing tube furnace. In order to improve the electronic conductivity, 10 wt% of ketchen black (LMB/C : KB) or sucrose (LMB/C : SC) was added in the starting

*Corresponding author:
Tel : +82-54-820-6272
Fax: +82-54-820-6211
E-mail: hlee@andong.ac.kr

powder and then the mixture was processed with the same procedure used for the pristine LiMnBO_3 .

The crystal structure and morphology of the sample were examined by X-ray diffraction (XRD, Rigaku D/MAX 2000 with $\text{Cu K}\alpha$ radiation) and scanning electron microscope (SEM, JSM-6700F, Jeol).

The working electrode was prepared from a mixture of 80 wt% active materials, 10 wt% Super P carbon black, and 10 wt% KF-1100 binder in an N-methyl-2-pyrrolidone (NMP) solvent. The slurries were coated onto aluminum foil, dried at 60°C , and roll pressed. Coin type half cells (CR2032) were constructed, in a dry room, with Li metal as a counter electrode, a Celgard 2400 as a separator, and LiPF_6 (1M) in a mixture of ethylene carbonate and ethylmethyl carbonate (EC/EMC, 1 : 2 in volume) as an electrolyte. The cells were galvanostatically charged and discharged at 15 mA/g over a voltage range of 1.0 - 4.8 V vs. Li^+/Li using a battery cycler (WonATech, WBCS3000).

Results and Discussion

LiMnBO_3 has two polymorphs. The low temperature form is monoclinic with C12/C1 in which trigonal-bipyramidal Li and Mn sites are separated into an upper site and lower site [19]. The high temperature form of LiMnBO_3 is hexagonal with P-6, where each MO_5 pyramid shares two opposite edges of its base with two pyramids, forming columns of edge sharing pyramids along c-axis [14]. Fig. 1 shows the XRD patterns of prepared powders. The peaks in Fig. 1(a) are mostly of monoclinic phase except some peaks marked as hexagonal. At 800°C of the firing temperature, the XRD pattern of pristine LiMnBO_3 , Fig. 1(b), shows only peaks of hexagonal phase, but both $\text{LiMnBO}_3/\text{C}:\text{KB}$ and $\text{LiMnBO}_3/\text{C}:\text{SC}$ have peaks of monoclinic phase, implying the added carbon sources hindered the transformation from monoclinic to hexagonal structure upon heating. Nonetheless, it can be seen that monoclinic is the main structure at the firing temperature of 500°C , while hexagonal structure is dominated at 800°C , which is in agreement with the previous reports [14, 19].

The SEM images, where morphological features of LiMnBO_3 and LiMnBO_3/C can be seen, are presented in Fig. 2. The pristine LiMnBO_3 fired at 800°C shown in Fig. 2(a) consists of isolated big particles with a size of about 4 ~ 5 μm , and the particle surface is very smooth which indicates that the excessive grain growth took place during firing. On the other hand, the SEM image of $\text{LiMnBO}_3/\text{C}:\text{KB}$ fired at 800°C (Fig. 2(b)) shows even particles with sizes of about 50 nm. Hence, it seems that the ketchen black in the starting powder not only played a role as a conductivity enhancer but also effectively suppressed the excessive grain growth occurred in the pristine of LiMnBO_3 . $\text{LiMnBO}_3/\text{C}:\text{SC}$ fired at 800°C is composed of uneven particles with a particle size ranging from ~ 100 to 700 nm in Fig. 2(c). Thus, it is likely that the sucrose also suppressed the

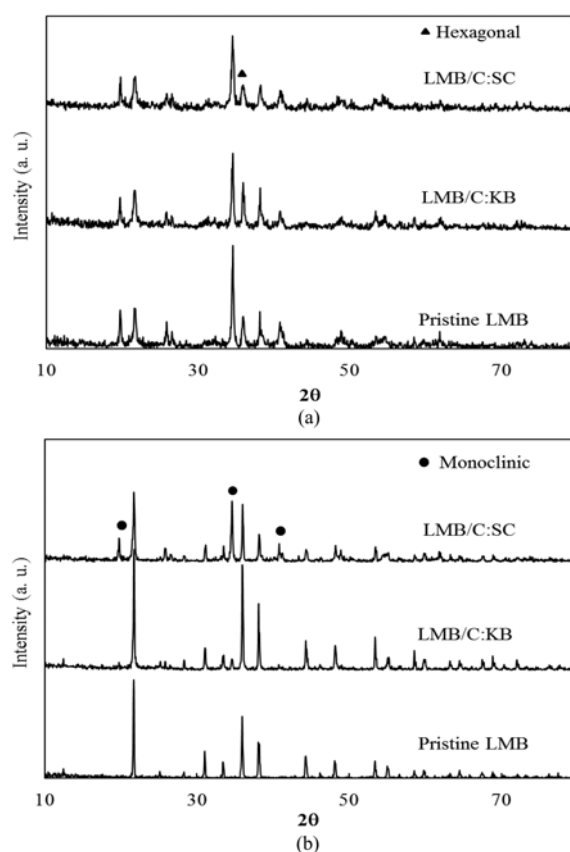


Fig. 1. XRD diffraction patterns of pristine LiMnBO_3 and LiMnBO_3/C fired at (a) 500°C and (b) 800°C .

excessive grain growth during firing but it was not as effective as the ketchen black. Unlike the ketchen black, which existed from the beginning, the sucrose was completely dissolved in the acetone at the beginning, and then decomposed into carbon coating on the LiMnBO_3 particles during firing. This might be the reason why the sucrose was not possible to suppress the grain growth effectively, since the formation of carbon coating would be completed at the relatively later stage and the material transport would be still possible through the thin carbon coating. The carbon content of the fired $\text{LiMnBO}_3/\text{C}:\text{SC}$ was measured to be ~ 3.8 wt%.

When the starting mixture was fired at 500°C , the excessive grain growth was not observed even in the pristine LiMnBO_3 owing to the less thermal energy. In Fig. 2(d-f), there is no big difference in size between samples, and the sizes of $\text{LiMnBO}_3/\text{C}:\text{KB}$ and $\text{LiMnBO}_3/\text{C}:\text{SC}$ particles are slightly smaller than those fired at 800°C . It is interesting to note that the morphology of pristine LiMnBO_3 particle shown in Fig. 2(d) looks like a rod shape while the $\text{LiMnBO}_3/\text{C}:\text{KB}$ and $\text{LiMnBO}_3/\text{C}:\text{SC}$ particles show more spherical morphologies, although the reason is not clear here.

The results of charge and discharge tests at 15 mA/g are shown in Fig. 3. Regardless of firing temperature, pristine LiMnBO_3 displays very low discharge capacities, which

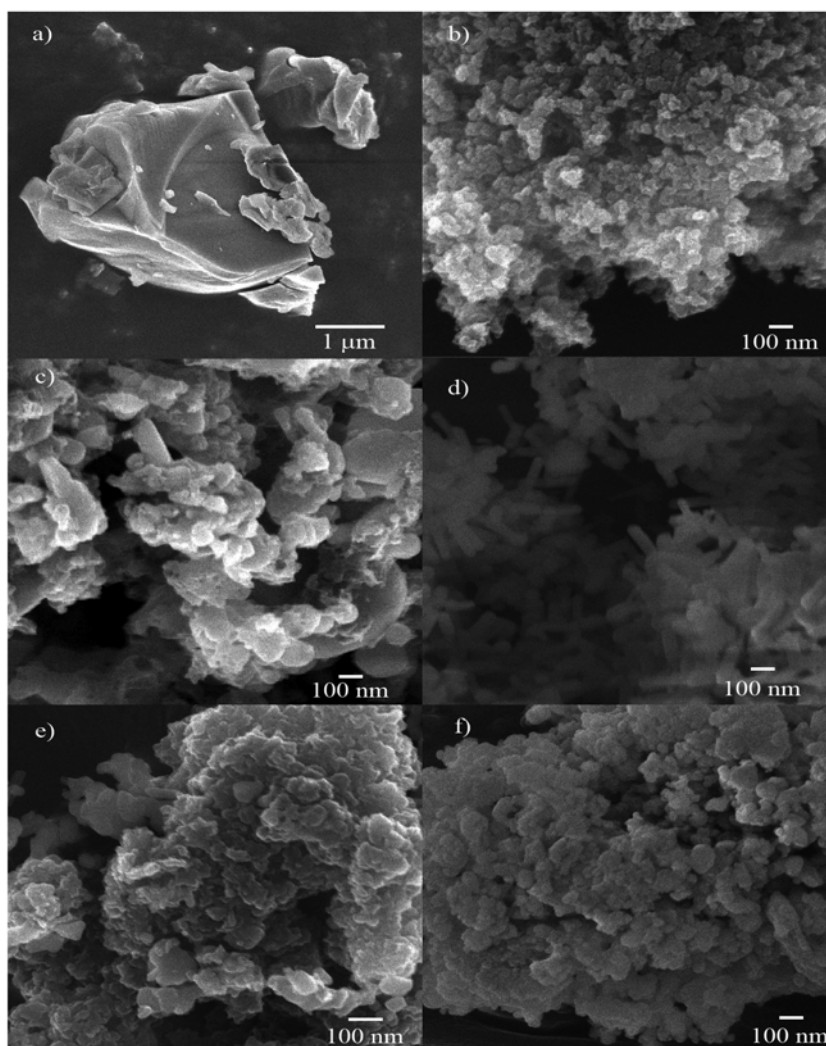


Fig. 2. SEM images of (a) pristine LiMnBO_3 fired at $800\text{ }^\circ\text{C}$, (b) $\text{LiMnBO}_3/\text{C}:\text{KB}$ fired at $800\text{ }^\circ\text{C}$, (c) $\text{LiMnBO}_3/\text{C}:\text{SC}$ fired at $800\text{ }^\circ\text{C}$, (d) pristine LiMnBO_3 fired at $500\text{ }^\circ\text{C}$, (e) $\text{LiMnBO}_3/\text{C}:\text{KB}$ fired at $500\text{ }^\circ\text{C}$, and (f) $\text{LiMnBO}_3/\text{C}:\text{SC}$ fired at $500\text{ }^\circ\text{C}$.

are less than 10 mAh/g at the 30th cycle. Among them, the LiMnBO_3 fired at $500\text{ }^\circ\text{C}$ has considerably higher initial discharge capacities, i.e., 58 mAh/g at the first and 38 mAh/g at the 5th cycles, than that fired at $800\text{ }^\circ\text{C}$. However, the discharge curve at the 10th cycle in Fig. 3(c) shows that more than 10 mAh/g of capacity was contributed from $1.0 - 1.3\text{ V}$ voltage window. Further, the discharge capacity of the pristine LiMnBO_3 fired at $500\text{ }^\circ\text{C}$ dropped very quickly after 10 cycles in Fig. 1(a). Because this low specific capacity of pristine LiMnBO_3 was mainly due to the low electronic conductivity, it could be expected that the incorporation of carbon into LiMnBO_3 would substantially enhance the capacity by improving the electronic conductivity. With the ketchen black in the starting powder ($\text{LiMnBO}_3/\text{C}:\text{KB}$), which led to the formation of $\text{LiMnBO}_3\text{-C}$ composite after firing, the discharge capacities at the first and the 30th cycles were 163 and 76 mAh/g , respectively, at the firing temperature of $500\text{ }^\circ\text{C}$, while they were 82 and 42 mAh/g at $800\text{ }^\circ\text{C}$. Moreover, the discharge curves in Figs 3(b) and (c) show small shoulders above 3.5 V ,

suggesting possible flat $\text{Mn}^{3+}/\text{Mn}^{2+}$ redox-potential at the high voltage range.

With the addition of sucrose in the starting powder ($\text{LiMnBO}_3/\text{C}:\text{SC}$), which resulted in the carbon coating on LiMnBO_3 particles, the discharge capacity improved as well, though not as good as the $\text{LiMnBO}_3\text{-C}$ composite, such that the discharge capacities at the 30th cycle were 23 and 15 mAh/g at 500 and $800\text{ }^\circ\text{C}$, respectively. This relatively weak electrochemical performance of the $\text{LiMnBO}_3/\text{C}:\text{SC}$, as compared to $\text{LiMnBO}_3/\text{C}:\text{KB}$, might be from the less amount of carbon content in the final product, i.e., 10 wt\% for $\text{LiMnBO}_3/\text{C}:\text{KB}$ and less than 5 wt\% for $\text{LiMnBO}_3/\text{C}:\text{SC}$, and/or poor carbon coating coverage on the particle surface. Further investigation is required to clarify this. Overall, the monoclinic LiMnBO_3 shows higher capacity than hexagonal counterpart. Even for the pristine LiMnBO_3 and $\text{LiMnBO}_3/\text{C}:\text{SC}$, which show similar capacities at the 30th cycle regardless of the firing temperature, the samples fired at $500\text{ }^\circ\text{C}$ have much higher initial capacity in Fig. 3(a), implying the greater

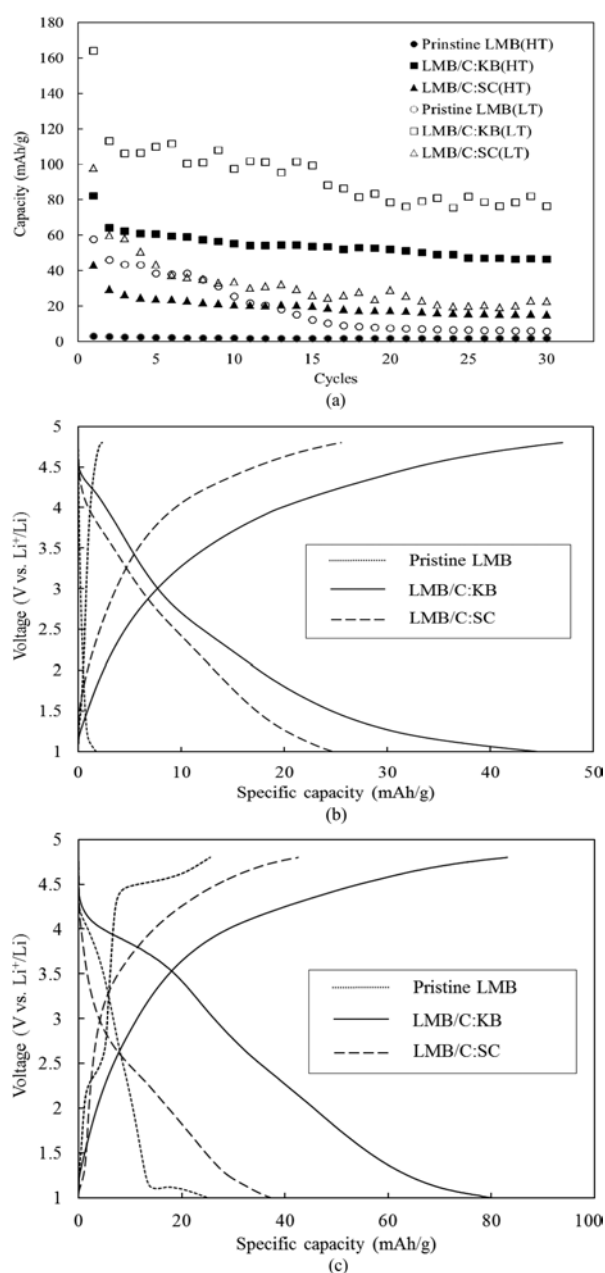


Fig. 3. (a) Discharge capacities of pristine LiMnBO_3 and LiMnBO_3/C fired at 800 (HT) and 500 °C (LT), (b) charge and discharge curves at the 10th cycle of specimens fired at 800 °C, (c) charge and discharge curves at the 10th cycle of specimens fired at 500 °C.

potential of monoclinic LiMnBO_3 for large capacity. This better lithium electrochemical performance of monoclinic LiMnBO_3 was also reported theoretically and experimentally in the previous study. The differences in the size, stability of the delithiated state, and lithium diffusion were pointed out as being responsible for the relatively poor performance of hexagonal LiMnBO_3 [18].

In summary, although the pristine LiMnBO_3 showed very limited lithium intercalation behavior, the carbon addition into LiMnBO_3 as a form of composite or coating substantially improved the lithium electrochemical performance of LiMnBO_3 . Further, monoclinic phase LiMnBO_3 showed better electrochemical performance

which was in good agreement with the previous studies.

Conclusions

The present study showed that the LiMnBO_3 could have a meaningful capacity when incorporated with carbon to enhance the electronic conductivity. Without carbon, the pristine LiMnBO_3 showed very small capacity after 30 cycles even with a wide voltage window. By incorporating carbon into LiMnBO_3 using a kitchen black or sucrose as a carbon source, the specific capacity increased up to 76 mAh/g at the 30th cycle for monoclinic LiMnBO_3 . Since the synthetic procedure in the present study has not polished yet, further improvement is expected by the optimized synthetic route for better control of morphology, phase, and the way of carbon addition.

Acknowledgements

This work was supported by a grant from 2010 Research Fund of Andong National University

References

1. T. Reddy, in "Linden's Handbook of Batteries" McGraw-Hill Professional (2010) 1.
2. A.K. Padhi, K.S. Nanjundaswamy, J.B. Goodenough, *J. Electrochem. Soc.* 144 (1997) 1188-1194.
3. P.G. Balakrishnan, R. Ramesh, T. Prem Kumar, *J. Power Sources* 155 (2006) 401-404.
4. F. Joho, P. Novak, M.E. Spahr, *J. Electrochem. Soc.* 149 (2002) A1020-A1024.
5. J.W. Fergus, *J. Power Sources* 195 (2010) 939-954.
6. B.L. Ellis, K.T. Lee, L.F. Nazar, *Chem. Mater.* 22 (2010) 691-714.
7. Y. Wang, G. Cao, *Adv. Mater.* 20 (2008) 2251-2269.
8. H. Song, K.T. Lee, M.G. Kim, L.F. Nazar, J. Cho, *Adv. Funct. Mater.* 20 (2010) 3818-3834.
9. B. Kang, G. Ceder, *Nature* 458 (2009) 190-193.
10. D. Choi, D. Wang, I.-T. Bae, J. Xiao, Z. Nie, W. Wang, V.V. Viswanathan, Y.J. Lee, J.-G. Zhang, G. Graff, Z. Yang, J. Liu, *Nano Lett.* 10 (2010) 2799-2805.
11. J. Kim, D.-H. Seo, S.-W. Kim, Y.-U. Park, K. Kang, *Chem. Commun.* 46 (2010) 1305-1307.
12. R. Dominko, *J. of Power Sources* 184 (2008) 462-468.
13. T. Muraliganth, K.R. Stroukoff, A. Manthiram, *Chem. Mater.* 22 (2010) 5754-5761.
14. V. Legaigneur, Y. An, A. Mosbah, R. Portal, A. Le Gal La Salle, A. Verbaere, D. Guyomard, Y. Piffard, *Solid State Ionics* 139 (2001) 37-46.
15. A. Yamada, N. Iwane, Y. Harada, S. Nishimura, Y. Koyama, I. Tanaka, *Adv. Mater.* 22 (2010) 3583-3587.
16. Y. Dong, Y.M. Zhao, Z.D. Shi, X.N. An, P. Fua, L. Chen, *Electrochim. Acta* 53 (2008) 2339-2345.
17. J.L. Allen, K. Xu, S.S. Zhang, T.R. Jow, *Mater. Res. Soc. Symp. Proc.* 730 (2002) V1. 8. 1.
18. J.C. Kim, C.J. Moore, B. Kang, G. Hautier, A. Jain, G. Ceder, *J. Electrochem. Soc.* 158 (2011) A309-A315.
19. O.S. Bondareva, M.A. Simonov, Y.K. Egorov-Tismenko, N.V. Belov, *Sov. Phys. Crystallo.* 23 (1978) 269-271.